

Non-Maxwellian Ion Energy Distribution in ECH-heated plasmas on TCV

A.N.Karpushov, B.P.Duval, T.P.Goodman, Ch.Schlatter

Ecole Polytechnique Fédérale de Lausanne (EPFL), Centre de Recherches en Physique des Plasmas, Association Euratom-Confédération Suisse, CH-1015 Lausanne, Switzerland

Introduction. This paper presents experimental results of the observation of a suprathermal ion population in the TCV tokamak, where the ion energy distribution was studied with Neutral Particle Analysers (NPAs) [1]. The flexibility of the TCV ECH system permitted an investigation of the dependence of the properties of the hot ion distribution on plasma and ECH parameters. Earlier experimental observations [2] are expanded with plasma current and density scans and the employment of a new "Compact Neutral Particle Analyser" (CNPA) featuring mass and energy separation over a broader energy range. The optimal experimental conditions for generation of suprathermal ions on TCV are found. These experiments extend the experimental database required for understanding the mechanisms of suprathermal ion generation [3].

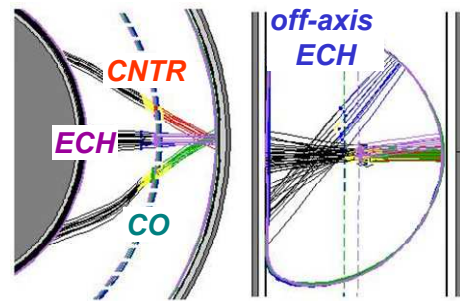


Fig.1: Gyrotrons alignment: ray-traces from TORAY calculation.

1. Experimental setup. These experiments, on the TCV Tokamak ($R=0.88$ m, $a=0.25$ m), employed the X2 (82.7 GHz) EC system, with a total delivered power of up to 2.0 MW (4 gyrotrons) in X-mode. In the reference plasma scenario, (optimal for generation of suprathermal ions), two gyrotrons were aligned for on-axis EC power deposition ~ 1 MW, where the real-time X2 mirror movement were used to change the toroidal injection angle (CNTR-pure ECH-CO ECCD), whilst the two other gyrotrons (~ 1 MW) were used to sustain an electron thermal barrier with deposition off-axis in pure ECH mode (Fig.1). The central electron density was $\sim 2 \times 10^{19} \text{ m}^{-3}$ ($1-4 \times 10^{19} \text{ m}^{-3}$ for density scans), the electron temperature reached 8 keV in regimes with eITBs and the plasma current was 140 kA (100-200 kA for I_p scan). The EC power deposition and current drive profiles are calculated by the TORAY ray-tracing code with magnetic equilibrium reconstruction from the LIUQE code and Thomson scattering electron temperature and density profiles. The total plasma energy content on TCV was calculated from the diamagnetic measurement. The ion energy content can be inferred as the

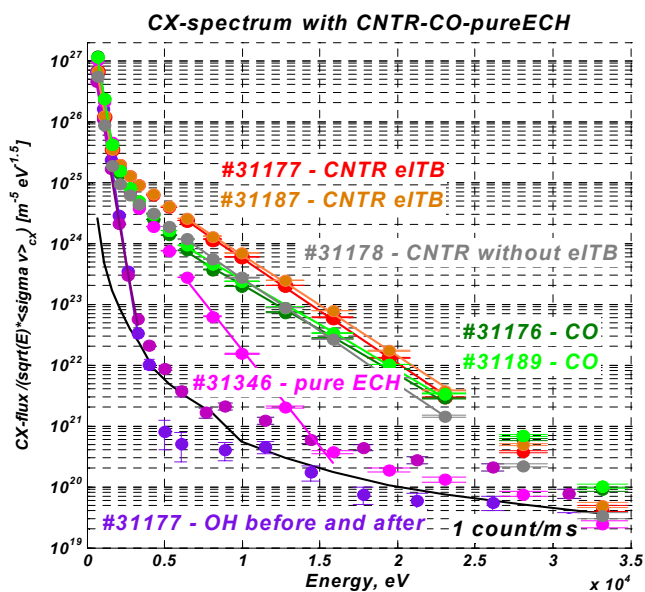


Fig.2: CNPA "CX-spectrums" in TCV plasma discharges with suprathermal ion populations.

difference between total plasma energy and the total electron energy from TS measurements.

The 28-channel "Compact Neutral Particle Analyzer" (CNPA) with mass and energy separation in $E \parallel B$ field simultaneously detects two mass species (11 channels for hydrogen and 17 for deuterium) in the 0.5-50 keV energy range with a time resolution 0.5-4.0 ms. The "Five-Channel Energy Atomic Particle Analyser" (5-ch.NPA) was operated in double electrical analysis mode with fast voltage sweeping, but no atomic mass discrimination covering the energy range 0.6-6.5 keV, with a time resolution of 1-13 ms. The DOUBLE-TCV numerical code was used to model the energy spectra of neutrals leaving the plasma and entering the NPAs.

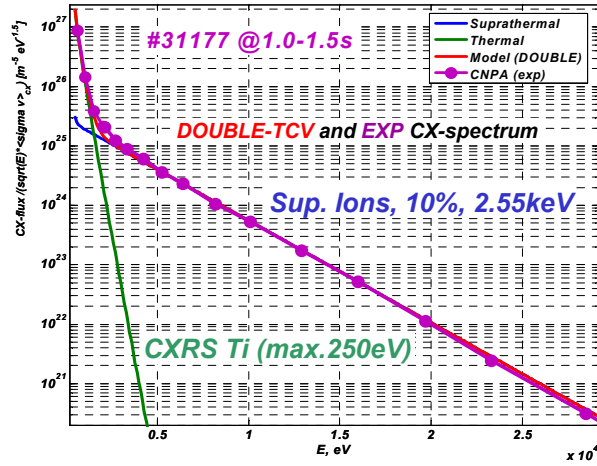


Fig.3: "CX-spectrum" in TCV plasma discharge with eITB and on-axis picked CNTR-ECCD deposition: experiment (CNPA) and DOUBLE-TCV modelling with $T_e(0)=7.1\text{keV}$, $n_e(0)=1.9 \times 10^{19} \text{m}^{-3}$, $T_i^T(0)=250\text{eV}$, $T_i^{\text{sup}}=2.55\text{keV}$, $n_i^{\text{sup}}/n_i^T=17\%$.

2. Bi-Maxwellian ion energy distribution in TCV ECH-heated plasma. The passive energy spectra of the atomic flux $J(E)$ emitted from the plasma into the NPA is the integral of fluxes in the plasma column along the line of sight (L) of the analyser. It may be expressed as:

$$J(E) = \Omega S \int_L n_a n_i f_i \langle \sigma_{cx} v_{ia} \rangle \gamma_{at} dl \quad [1].$$

The "CX-spectra"

$F_{dc}(E) = J(E) / (\sigma_{cx}(E) \times E)$ for different plasma and ECH conditions are shown in Fig.2. For low density plasmas with a Maxwellian ion energy distribution, the ion temperature should be proportional to the logarithm of the F_{dc} slope (Fig.2 – OH plasma with $T_i=250-260 \text{ eV}$). For more complicated plasmas the DOUBLE-TCV code was used to interpret the NPA measurements. The "CX-spectra" measured during TCV ECH-heated discharges with suprathermal ions can be reasonably modelled by assuming two ion populations. An example the "CX-spectrum" measured by CNPA and results of DOUBLE-TCV modelling with a thermal bulk ($T_i^T \sim 250 \text{ eV}$) and a suprathermal component with an effective temperature ($T_i^{\text{sup}}=2.55 \text{ keV}$) is shown in Fig.3. We use the suprathermal ion effective temperature (T_i^{sup}), density (n_i^{sup}/n_i^T) and energy (W_i^{sup}/W_i^T) ratios of suprathermal and bulk ion populations as a quantitative characterisation of the suprathermal ion population.

The strongest effect on the suprathermal ion population was observed in eITB plasmas with an on-axis electron density of $1.7-2.1 \times 10^{19} \text{ m}^{-3}$, plasma current 140 kA and peaked on-axis CNTR-ECCD (20 MW/m^3 , -5 MA/m^3). The measured neutral flux indicates a density of suprathermal ions $\sim 10-30\%$ of the thermal ion density with the energy content in the suprathermal ions up to a few times higher than bulk ion energy content. The carbon impurity C^{VI} ion temperature from CXRS [4] technique was close to the thermal deuterium bulk temperature from NPA measurements. The suprathermal ion population was a few times lower in the discharges without eITB with electron temperatures of 4-5 keV (in

contrast to 7-8 keV with eITB), and the difference between CO and CNTR-ECCD discharges may be related to changes in the plasma energy confinement.

3. Scans of EC deposition radius, plasma current and density. Parameters of the suprathermal ion population were observed to be sensitive to the EC deposition position and toroidal injection angle. The non-Maxwellian ion feature is not observed when the deposition location is placed outside the sawtooth inversion radius [2]. The transition of ECCD deposition through ρ_{inv} ($\rho=0.17$ in Fig.4) leads to a decrease of the electron temperature and destroys the conditions necessary for generation of suprathermal ions.

A decrease of the suprathermal ion density was observed with increasing plasma current (Fig.5,6). For the plasma currents higher than ~ 155 kA the ‘‘CX-spectrum’’ could not be fitted with a bi-Maxwellian ion energy distribution assumption (green points in Fig.6).

The characteristics of suprathermal ions are also sensitive to the plasma density. The energy content, density and temperature of the suprathermal ion population decrease with plasma density (Fig.7). The linear density of $1 \times 10^{19} \text{ m}^{-2}$, limited by the machine wall recycling, was the lowest accessible in TCV. The ‘‘CX-spectrum’’ for the plasma density scan was well modeled by bi-Maxwellian ion energy distribution.

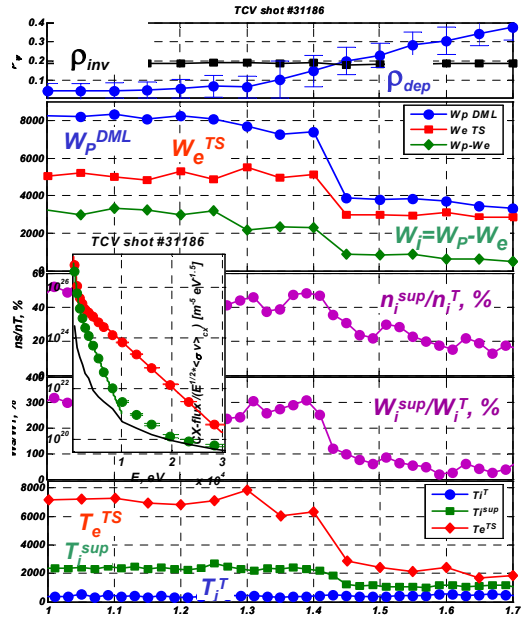


Fig.4: Parameters of the suprathermal ions in the TCV discharge with ramp-down the toroidal magnetic field. The decrease of magnetic field from 1.42 to 1.24 T leads to the shift of EC deposition from 0.03 to 0.40 in ρ_{ψ} .

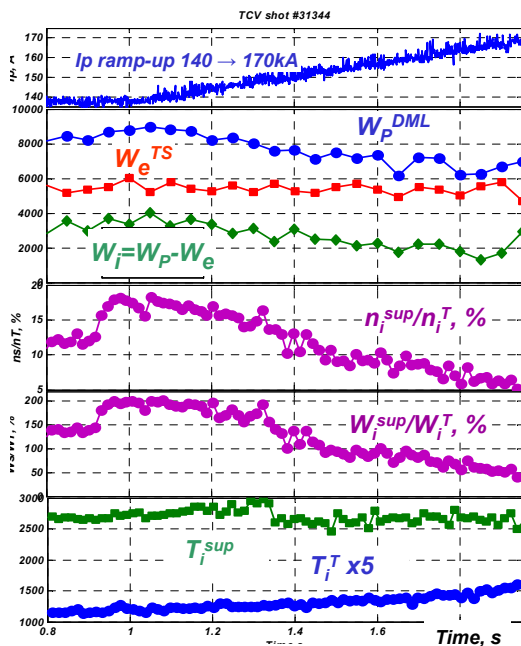


Fig.5: Plasma parameters in the TCV discharge with plasma current ramp-up.

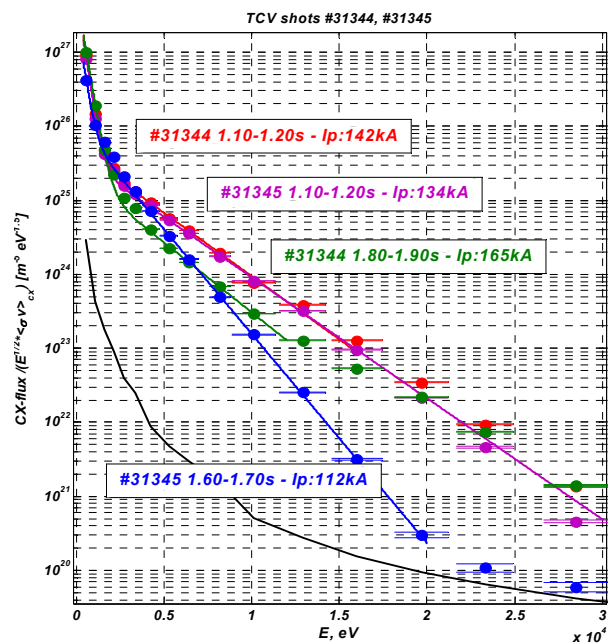


Fig.6: ‘‘CX-spectrums’’ for different plasma current.

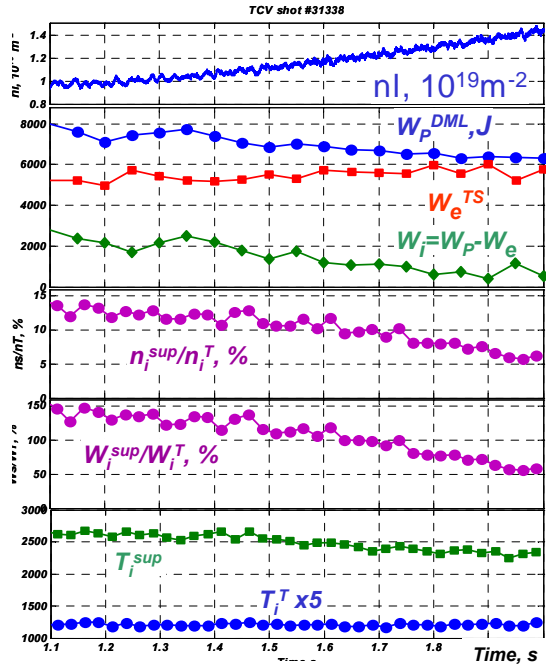


Fig.7: Plasma parameters in the TCV discharge with plasma density ramp-up.

populations thus causing efficient anomalous energy transfer from the electrons to the ions. The suprathermal electron population with a density of a few percent and energies up to a few 100 keV has been measured by the ECE diagnostic during optimal suprathermal ion generation conditions. The link between bulk electron temperature and the parameters of suprathermal ions confirms the importance of the electron energy distribution for energy transfer from electrons to ions.

4. Discussion. The generation of suprathermal ions may not be explained by the classical theory of two-body Coulomb collisions. Additional anomalous wave-ion [5] or electron-ion coupling [6] effects will have to be considered to understand this phenomenon. The mechanism responsible for this effect remains an open question.

The experimental observation of the non-Maxwellian features on the ion energy distributions in the ECH heated TCV plasma are not inconsistent with the mechanisms resulting in the slide-away regime of the electron energy distribution [3]. Powerful on-axis ECCD leads to the formation of an electron energy distribution of which a considerable fraction tends to a slide-away. Modes in the lower-frequency ($\omega^2 \leq \omega_{pi}^2$) could resonate both with the electron and ion

References:

1. Karpushov A.N., et al., "Neutral particle analyzer diagnostics on the TCV Tokamak", Rev. Sci. Instrum. 77, 033504 (2006).
2. Karpushov A.N., Coda S., Duval B.P., "Observation of suprathermal ions in the TCV during ECH and ECCD", Proc. 30th EPS Conference on Controlled Fusion and Plasma Physics, St Petersburg, Russia, July 2003, ECA Vol. 27A, P-3.123
3. Schlatter Ch., et al., "Conditions for anomalous energy and momentum transfer from electrons to ions in ECCD discharges on TCV", this conference (2006), P-1.149.
4. Bosshard P., Duval B.P., Karpushov A., Mlynar M. , "Ion Temperature Behaviour and Ion Contribution to the Power Balance Measured by CXRS in Ohmic and ECR Heated Plasmas on TCV" , Proc. 29th EPS Conference on Controlled Fusion and Plasma Physics, Montreux, Switzerland, June 2002, ECA Vol. 26B (2002) (P-4.120).
5. Erckmann V. and Gasparino U., "Electron cyclotron resonance heating and current drive in toroidal fusion plasmas", *Plasma Phys. Control. Fusion* 36, (1994) 1896-1962
6. Coppi B.; Pegoraro F.; Pozzoli R.; Rewoldt G., "Slide-away distributions and relevant collective modes in high-temperature plasmas" *Nucl. Fusion* 16(2), (1976) 309-328

This work was partly supported by the Swiss National Science Foundation.